Journal of Cellular Biochemistry 103:941–956 (2008)

Characterization of Apin, a Secreted Protein Highly Expressed in Tooth-Associated Epithelia

Pierre Moffatt,[2,3] Charles E. Smith,[1] René St-Arnaud,[2,3] and Antonio Nanci[1]*

[1]Laboratory for the Study of Calcified Tissues and Biomaterials, Département de Stomatologie, Faculté de Médecine Dentaire, Université de Montréal, Montréal, Québec, Canada H3C 3J7
[2]Genetics Unit, Shriners Hospital for Children, Montréal, Québec, Canada H3G 1A6
[3]Department of Human Genetics, McGill University, Montréal, Québec, Canada H3A 2T5

Abstract We previously reported expression of a protein by enamel organ (EO) cells in rat incisors, originally isolated from the amyloid of Pindborg odontogenic tumors called Apin. The aim of the present study was to further characterize the Apin gene and its protein in various species, assess tissue specificity, and clarify its localization within the EO. Northern blotting and RT-PCR revealed that expression of Apin was highest in the EO and gingiva, moderate in nasal and salivary glands, and lowest in the epididymis. The protein sequences deduced from the cloned cDNA for rat, mouse, pig, and human were aligned together with those obtained from four other mammal genomes. Apin is highly conserved in mammals but is absent in fish, birds, and amphibians. Comparative SDS–PAGE analyses of the protein obtained from bacteria, transfected cells, and extracted from EOs all indicated that Apin is post-translationally modified, a finding consistent with the presence of predicted sites for phosphorylation and O-linked glycosylation. In rodent incisors, Apin was detected only in the ameloblast layer of the EO, starting at post-secretory transition and extending throughout the maturation stage. Intense labeling was visible over the Golgi region as well as on the apices of ameloblasts abutting the enamel matrix. Apin was also immunodetected in epithelial cells of the gingiva which bind it to the tooth surface (junctional epithelium). The presence of Apin at cell-tooth interfaces suggests involvement in adhesive mechanisms active at these sites, but its presence among other epithelial tissues indicates Apin likely possesses broader physiological roles. J. Cell. Biochem. 103: 941–956, 2008.

Key words: enamel organ; junctional epithelium; basement membrane; ameloblast; tooth; secreted protein; gingiva

Tooth enamel formation is a tightly regulated process in which epithelial cells called ameloblasts express a limited but important set of genes encoding for certain secreted proteins. Gene knockout experiments have shown that at least four independent tooth-specific gene products, three extracellular matrix proteins (amelogenin, ameloblastin, enamelin) and one enzyme (enamelysin, MMP-20) are essential for normal enamel formation [Gibson et al., 2001; Caterina et al., 2002; Fukumoto et al., 2004; Masuya et al., 2005]. In all cases, dramatic phenotypes have been observed in these mouse models ranging from mild hypoplasia (MMP-20-deficient) to near complete absence of enamel (ameloblastin-deficient), mimicking forms of the human disease condition called amelogenesis imperfecta [Wright, 2006]. Kallikrein 4 is another enzyme that has been shown to be critical for normal enamel formation and that has also been linked to amelogenesis imperfecta in humans [Hart et al., 2004]. Such experiments demonstrate that enamel matrix proteins cannot mutually compensate for the loss of any single member, an expected outcome considering that each of these proteins possesses unique physicochemical properties [Smith, 1998; Bartlett et al., 2006]. For instance, it is generally accepted that amelogenins occupy spaces between crystals and regulate their growth in width and thickness, while newly secreted ameloblastin and enamelin are present only at the forming enamel surface, are short lived, and likely have

Grant sponsor: Canadian Institutes of Health Research; Grant number: MOP-68826.

*Correspondence to: Antonio Nanci, PhD, Université de Montréal, Faculté de Médecine Dentaire, PO Box 6128, Station Centre-Ville, Montréal, Québec, Canada H3C 3J7. E-mail: antonio.nanci@umontreal.ca

Received 30 March 2007; Accepted 6 June 2007

DOI 10.1002/jcb.21465

some role in regulating crystal elongation [Moradian-Oldak et al., 2000]. The precise mechanisms by which these proteins exert their function(s), however, remain to be elucidated.

Other genetically altered mouse models for more widely expressed proteins such as laminin alpha3 [Ryan et al., 1999], connexin43 [Flenniken et al., 2005], cystic fibrosis transmembrane conductor [Sui et al., 2003], periostin [Rios et al., 2005], and urokinase-type plasminogen activator [Miskin et al., 2006], display defects in tooth and enamel formation and highlight the interplay of many different and less appreciated proteins in this process. In this context, we have undertaken a broad screening for secreted proteins using a rat incisor enamel organ (EO) library and recently identified two novel proteins, amelotin (Amtn) and Apin, produced by ameloblasts during the maturation stage of amelogenesis, a critical time for final developmental hardening of the enamel layer [Moffatt et al., 2006a]. Amtn [Iwasaki et al., 2005; Moffatt et al., 2006b] and Apin [Moffatt et al., 2006a; Solomon et al., 2003] are encoded by two different genes categorized solely on their genomic location and architecture as members of the secretory calcium-binding phosphoprotein gene cluster [Kawasaki and Weiss, 2003, 2006; Huq et al., 2005]. These genes encode a number of structurally diverse proteins that stabilize Ca and PO_4 ions in body fluids and/or guide $CaPO_4$ deposition onto receptive extracellular matrices. Immunolocalizations have shown that Amtn is associated with the basal lamina at the interface between the enamel surface and maturation stage ameloblasts as well as junctional epithelium (JE) [Moffatt et al., 2006b]. Since these epithelia are tightly bound to the tooth surface, a putative cell adhesion role has been inferred for Amtn based on this discrete localization [Moffatt et al., 2006b]. The JE is a specialized structure that seals off the tooth from the oral cavity, and loss of its integrity is the first step towards periodontal diseases with ensuing bone and tooth loss [Kinane et al., 2005].

There is presently relatively little information about Apin apart from data showing that it is expressed at high levels in maturation stage EOs of rodents [Moffatt et al., 2006a]. Apin contains a cleavable signal peptide and an abundance of glutamine and proline residues [Moffatt et al., 2006a], but it does not possess any recognizable motifs or domains that give insights into its function or activity. Furthermore, Apin does not have any related family members. Previous studies, all based on a transcriptomic approaches but using different identification strategies, have isolated Apin cDNA fragments from various sources such as lachrymal glands [Ozyildirim et al., 2005], tongue [The FANTOM Consortium, 2005], and tooth [Bonass et al., 1998; Dey et al., 2001]. More recently, DNA microarray analyses have shown that Apin is upregulated in cancers of the cervix that harbor an activating mutation in FGFR3b [Rosty et al., 2005]. Furthermore, SAGEmap data [Lal et al., 1999] have provided evidence that Apin is the most upregulated gene (200-fold) in some gastric cancers [Aung et al., 2006]. Consistent with its expression in teeth [Moffatt et al., 2006a], C-terminal fragments of Apin have also been isolated from amyloid-like deposits present in human calcifying epithelial odontogenic tumors (CEOT) [Solomon et al., 2003]. CEOT are rare benign neoplasms that are believed to originate mainly from unerupted teeth [Philipsen and Reichart, 2000]. Whether the overexpression of Apin observed in various forms of cancer is causative or just coincidental, and whether this information has some prognostic or diagnostic significance, remains to be established.

The association of major Apin expression with enamel maturation suggests a possible important role for this protein in the final phases of tooth formation. However, the identity of the cell(s) expressing Apin in the EO, the site in the maturation stage of amelogenesis where the secreted protein accumulates, and whether JE co-express Apin along with Amtn are still unresolved questions. The present work was undertaken to address these issues as well as survey a broad range of tissues for Apin expression, and gain a more comprehensive overview of Apin produced in rat, mouse, human, and pig.

MATERIALS AND METHODS

Cell Culture

All culture media were supplemented with 10% (v/v) fetal bovine serum. The mouse chondrocytic (ATDC5), osteoblastic (MC3T3-E1-subclone 4), and ameloblast (LS8, kind gift from Dr. Malcolm S. Snead, UCS) cell lines were cultured in DMEM-F12, αMEM and DMEM,

respectively. The rat osteosarcoma cell lines UMR106 and ROS17/2.8, and the human HeLa and HEK293 (human embryonic kidney) cells were grown in DMEM. The human gastric carcinoma KATOIII cells were grown in RPMI1640. MC3T3 cells were also grown for various length of time (2, 7, 16, and 28 days) under conditions promoting their mineralization (αMEM supplemented with 10% FBS, 100 μg/ml ascorbic acid, and 3 mM β-glycerophosphate). Culture media were replenished every 2–3 days.

RNA Extraction and Cloning of Mouse, Human, and Pig Apin

Total RNA was extracted from selected adult tissues and cultured cells using Trizol (Invitrogen, Burlington, ON, Canada). The coding portion of the mouse and human Apin cDNA was amplified using the SuperScript™ III-Platinum Taq One-Step RT-PCR System (Invitrogen) with species-specific forward (mouse 5′-AGGTATACCATCTGAAAATG-3′; human 5′-CTAGATATATCATACGAAAATG-3′) and reverse primers (mouse 5′-TCTCCCAAAACTTCCAAGTG-3′; human 5′-GGCAACTTCTTATGGTTCCC-3′). Typically, 25 μl RT-PCR reactions contained 250 ng of total RNA from mouse mandible or from human KATOIII cells and were set up as per the manufacturer instructions. Following RT at 48°C/30 min and initial denaturing at 94°C/2 min, cycling conditions were 94°C/30 s, annealing at 50°C/30 s, elongation at 68°C/55 s (25 and 35 cycles for mouse and human cells, respectively), and a final step at 68°C/5 min. The mouse 873 bp and human 868 bp PCR products were separated on 1% agarose gels, purified on Minelute (QIAGEN, Mississauga, ON, Canada), and T/A cloned into the EcoRV site of pBluescriptKS (Stratagene, La Jolla, CA). Sequences for mouse (EF123456) and human (EF123456) Apin have been deposited to GenBank. Cloning of the pig full length cDNA was performed in two steps using total RNA obtained from the EO of 6-month-old pig 3rd molars (generous gift of Dr James P. Simmer, University of Michigan). First, mRNA was reverse transcribed with a dT_{15}-tailed oligo using Superscript II as described previously [Thomas et al., 2003]. The resulting single stranded cDNAs were used in a PCR reaction with the following degenerate primers that were designed from the coding portion of existing sequences from seven species: forward 5′-AAAATGARAAHYMTAATTCTTCTYGG-3′, reverse 5′-GTGCTKGGTKTTKGTGAIGTYGWIGG-3′. The pig Apin cDNA was amplified for 35 cycles with rTaq (New England BioLabs, Pickering, ON, Canada) as follows: 94°C for 30 s, 50°C/30 s, 72°C/50 s and a final step at 72°C/5 min. The PCR product was cloned in pBluescript as described above and sequenced. Based on the sequence obtained, a third pig-specific internal forward primer was designed (5′-TGACAGCAGAAGTGTTACCG-3′) and used in another PCR reaction along with the oligo (5′-GAGATGAATTCCTCGAGC-3′) complementary to the tail of the dT15-primer. The amplification product was cloned, sequenced, and the full length composite pig Apin cDNA deduced (GenBank acc. number DQ980195).

Northern Blotting and RT-PCR

Total RNA was extracted and electrophoresed on MOPS-buffered 1.1% agarose/1.2% formaldehyde gels. RNAs were transferred onto positively charged nylon membranes (Roche, Laval, QC, Canada) with 20× sodium citrate saline (SSC) buffer overnight, and fixed by UV crosslinking. Integrity of the RNAs was monitored by staining of blots with methylene blue [Wilkinson et al., 1991]. The blots were prehybridized for 2 h in Church buffer [Church and Gilbert, 1984] at 65°C and then hybridized overnight under the same conditions with species-specific Apin cDNA fragment. The rat Apin cDNA was obtained previously [Moffatt et al., 2006a]. Probes were labeled by random-priming with High Prime (Roche) and α^{32}P-dCTP (GE Healthcare, Baie d'Urfe, QC, Canada). After stringent washes with 0.2X SSC/0.1% SDS buffer at 65°C, blots were exposed to Kodak XA-R films. In some cases, the Northern results were validated by RT-PCR. Reactions were set up as described above using 250 ng of total RNA and the SuperScript™ III-Platinum Taq One-Step RT-PCR System (Invitrogen). Rat Apin forward (5′-CCTTCAACTCCTGGATTCC-3′) and reverse (5′-GAGTTTCTGGAGCTGTGCC-3′) primers were designed from exon 5 and 9, respectively. The human Apin forward (F2: 5′-AGCGTCTCATGTCTGCCAG-3′; F3: 5′-GAGGACAGCAGCAACTAGC-3′) and reverse (R1: 5′-ACTCCTGCACTGTCATGTC-3′; R2: 5′-GGCAACTTCTTATGGTTCCC-3′) primers were designed from various location within the gene but always encompassing at least 2 exons as schematized in Figure 2B. Glyceraldehyde

3-phosphate dehydrogenase (Gapdh) and Amtn primers used in parallel reactions were exactly as described previously [Moffatt et al., 2006b]. Typical RT-PCR conditions for the human were: 55°C/30 min, 94°C/2 min, 94°C/30 s, 50°C/30 s, 68°C/55 s.

Generation of an Antibody Against Recombinant Rat Apin

An NheI (blunted with Klenow)-XhoI fragment of the rat Apin full length cDNA was cloned into bacterial expression vector pQE31 (QIAGEN) that had been previously digested with BamHI (blunted with Klenow)-SalI. The ensuing construct expresses an Apin protein fragment, hereafter named r6His-rApin, consisting of 252 amino acids starting at S27 and extending to its stop codon. Fused to its N-terminus, is the pQE31 derived 6-histidine tag (MRGSHHHHHHTDPS) (see Fig. 4A). The plasmid was transformed into the M15 strain (QIAGEN), bacteria were grown to an OD of 600, and production induced for 5 h by addition of 1 mM isopropylthio-β-D-galactoside. The bacterial pellet was resuspended in lysis buffer (LB) (50 mM NaH_2PO_4, 300 mM NaCl, 20 mM imidazole, pH 8.0) at 4°C and sonicated. The lysate was centrifuged at 12,000 rpm and the r6His-rApin protein present in the soluble extract was bound on a nickel-nitriloacetic acid (Ni-NTA)-agarose affinity resin (QIAGEN) at room temperature. After washing the resin with 10 volumes of LB, the protein was eluted with LB containing 250 mM imidazole. Collected fractions were assessed for protein content using the Bradford assay and analyzed by SDS–PAGE gels and Coomassie blue staining. Fractions containing r6His-rApin were pooled concentrated on a 30 kDa cutoff Amicon Centricon unit (Millipore, Mississauga, ON, Canada) and desalted on PD-10 columns (GE Healthcare). The mass of the final r6His-rApin preparation was determined by LC-MS using an 1100 LC system coupled to an ESI-MSD-TOF mass spectrometer (Agilent Technologies, Mississauga, ON, Canada). The chromatographic column was a Poroshell 300SB-C8, heated at 45°C and operated at 0.2 ml/min. A linear gradient of 0.1% formic acid in acetonitrile for a total run time of 20 min was used for elution. The mass spectrometer was operated in positive electrospray mode and mass spectra were acquired from m/z 110 to 2000. Bioconfirm software (Agilent Technologies) was used to deconvolute the pattern of charge-state distributions of protein electrospray spectra. The recombinant protein was mixed with complete Freund's adjuvant and injected into rabbits according to standard protocols (Affinity BioReagents, Golden, CO).

Transient Transfection, Immunofluorescence, and Western Blotting

For expression of Apin in cells, the cDNA coding portions for mouse, human, and pig were sub-cloned into a CMV-based expression vector. The rat Apin cDNA original clone [Moffatt et al., 2006a] was modified by PCR to incorporate a unique AscI site at its 3′-end. A double stranded primer-linker with compatible overhangs was then inserted at the AscI site to produce a 13 residue extension (GADYKDDDDKGAP) that code for the FLAG epitope (underlined) fused at the rat Apin C-terminus. The corresponding untagged rat Apin sequence had a 3 amino acid extension (Gly-Ala-Pro) created by the AscI restriction site. The empty vector (mock) and one expressing green fluorescent protein (GFP) were used as controls to monitor transfection efficiency. Plasmid DNA was transiently transfected into HEK293 and HeLa cells using Fugene6 (Roche) and processed for the detection of overexpressed Apin proteins exactly as described [Moffatt et al., 2004]. Briefly, cells grown on cover slips were processed for immunofluorescence after fixing with 2% paraformaldehyde in PBS and with or without permeabilization in Triton X-100. All incubations and blocking were performed for 1 h each at 23°C in PBS containing 1% non fat milk and 0.5% BSA. The anti-r6His-rApin antiserum or its matching pre-immune serum were used at 1:5,000, and the secondary goat-anti-rabbit-Alexa594 was diluted 1:500. Nuclei were stained with 5 μg/ml Hoechst 33342 (Molecular Probes/Invitrogen) in PBS and the samples were mounted with ProLong Gold antifade reagent (Molecular Probes/Invitrogen). Fluorescence was examined under a Zeiss Axiophot microscope (Carl Zeiss Canada) equipped with an Olympus DP70 digital camera. For Western blotting, conditioned media and cell extracts were separated on 10% SDS–PAGE gels under reducing conditions and transferred to nitrocellulose. The blots were probed with the rabbit anti-Apin antiserum at 1:2,500, a chicken anti-amelogenin purified IgY [Orsini et al., 2001] at 1:1,000, or a mouse monoclonal anti-actin IgG

(clone mAbGEa, Affinity BioReagents) at 1:10,000, all in PBS-Tween 0.1% with 5% non fat milk. The species-specific secondary horseradish peroxidase conjugated antibodies (Sigma, St. Louis, MO) were used 1:30,000. The signal was visualized by chemiluminescence using ECL reagent (GE Healthcare).

Immunolocalizations and Western Blot Detection of Apin in Rat Tissues

Mandibles and maxillae, as well as samples of liver, stomach, spleen, heart, pancreas, kidney, brain, intestine, testis, lung, nasal, and salivary glands from male Wistar rats and CD1 mice were removed, fixed and processed for paraffin embedding as described previously [Moffatt et al., 2006b]. Deparafinized sections (5 μm) were blocked in PBS containing 5% skim milk for 1 h. Sequential incubations with the Apin antiserum or pre-immune serum followed by a secondary goat-anti-rabbit-AlexaFluor 594 antibody (Molecular Probes/Invitrogen) were performed at 1:500 dilutions in PBS at room temperature for 3 and 1 h respectively. Some sections were also similarly incubated with rabbit anti-Amtn antibody [Moffatt et al., 2006b] at 1:500 dilution. Following each incubation, the slides were washed three times for 10 min each with PBS-Tween (0.05% (v/v)). Nuclei were stained with Hoechst and the sections were mounted in ProLong Gold and observed as detailed above. For Western blots, various tissues were removed from 100 g male Wistar rats, snap frozen in liquid nitrogen, and lyophilized. Enamel organs strips corresponding to the secretory and maturation stages were dissected from freeze dried mandibular incisors [Smith et al., 2006]. The maturation stage samples were further separated into apical (adjacent to the secretory stage) and incisal (more mature) segments. All tissue samples were homogenized directly in 2× Laemmli buffer, boiled for 5 min, and loaded on 10% SDS–PAGE gels and processed as described above.

RESULTS

Expression Profile of Apin by Northern Blotting and RT-PCR

In order to determine the expression pattern of the Apin gene in rat, mouse, human, and pig, and to compare their protein sequences, full length cDNAs were first cloned by RT-PCR. Species-specific primers flanking the entire coding region were designed from the available mouse sequence (XM_132137), and from the predicted human cDNA deduced from the genome (Ensembl) after Blast homology search with our rat full length clone (DQ198380). As there are presently no data on pig Apin in existing databases, its cDNA was obtained in two steps with degenerate and internal sequence-specific primers. The starting RNA for mouse and pig were the whole mandible and isolated EO, respectively. For the human, the KATOIII gastric carcinoma cell line was used because partial ESTs had previously been obtained from this source (UniGene Hs.143811). The cloned sequences have been deposited to GenBank (human EF113908, pig DQ980195, mouse EF113909). Northern blot analyses were performed using as probes the coding portions of species-specific cDNAs. For the rat, robust Apin expression was detected using as little as 0.3 μg of RNA samples from EO and whole mandible (Fig. 1A). Expression was also found at lower levels in nasal and salivary glands (Fig. 1A). A much weaker signal was also observed in the epididymis upon longer autoradiographic exposures (Fig. 1A, middle panel). All other tissue tested and the osteosarcoma cell lines UMR106 and ROS17/2.8 were negative. Considering the amounts of RNA loaded, it can be estimated that expression levels in nasal and salivary glands were between 50- and 100-fold less than those in the EO or mandible. Also, the sizes of the mRNA transcripts in the former appeared slightly larger than those in the EO, possibly arising as alternative splicing of UTR exons. Like in rat, two bands were visible in pig EO with the smaller being expressed at higher levels (Fig. 1B). This smaller transcript likely corresponded to the full length mRNA migrating at roughly the same size as that for mouse Apin which was loaded as a positive control. The larger transcript likely arises as a result of alternative polyadenylation signal usage and consequently possesses a longer 3′UTR. The mouse Apin transcript was detected with a much weaker signal intensity when the pig probe was used (Fig. 1B). Among all mouse tissues and cell lines tested, only mandible gave a specific signal (Fig. 1C). Even the immortalized ameloblast-like cells LS8 [Chen et al., 1992] were negative for Apin (Fig. 1C). In the human cell lines, expression was detected in KATOIII and unexpectedly in HEK293 (Fig. 1D). The

transcript sizes were slightly different between the two cell lines, and HEK293 cells produced fainter signals at higher ranges (Fig. 1D). RT-PCR performed with RNA sampled from various rat tissues confirmed the Northern data and identified gingiva as an additional site for substantial expression of Apin (Fig. 2A). In all positive tissues tested (mandible, nasal glands, salivary glands, epididymis, gingiva) a unique 492 bp product was detected (Fig. 2A). In contrast, Amtn expression was restricted to mandible and gingiva (Fig. 2A). To explore the differences in the human Apin transcript sizes observed by Northern between KatoIII and HEK293 cells (Fig. 1D), various primer pairs were designed and used for RT-PCR as depicted in Figure 2B. Only KATOIII cells yielded the expected products (Fig. 2B) suggesting that Apin transcripts detected by Northern in HEK293 cells are either aberrant or non-specific.

Conservation of Apin Features Among Mammals

The mammalian Apin sequences derived from cloned cDNAs (human, mouse, pig, rat) were aligned to those deduced from genomic data (chimp, macaque, dog, cow; Fig. 3). At the genomic level, all species possessed the same

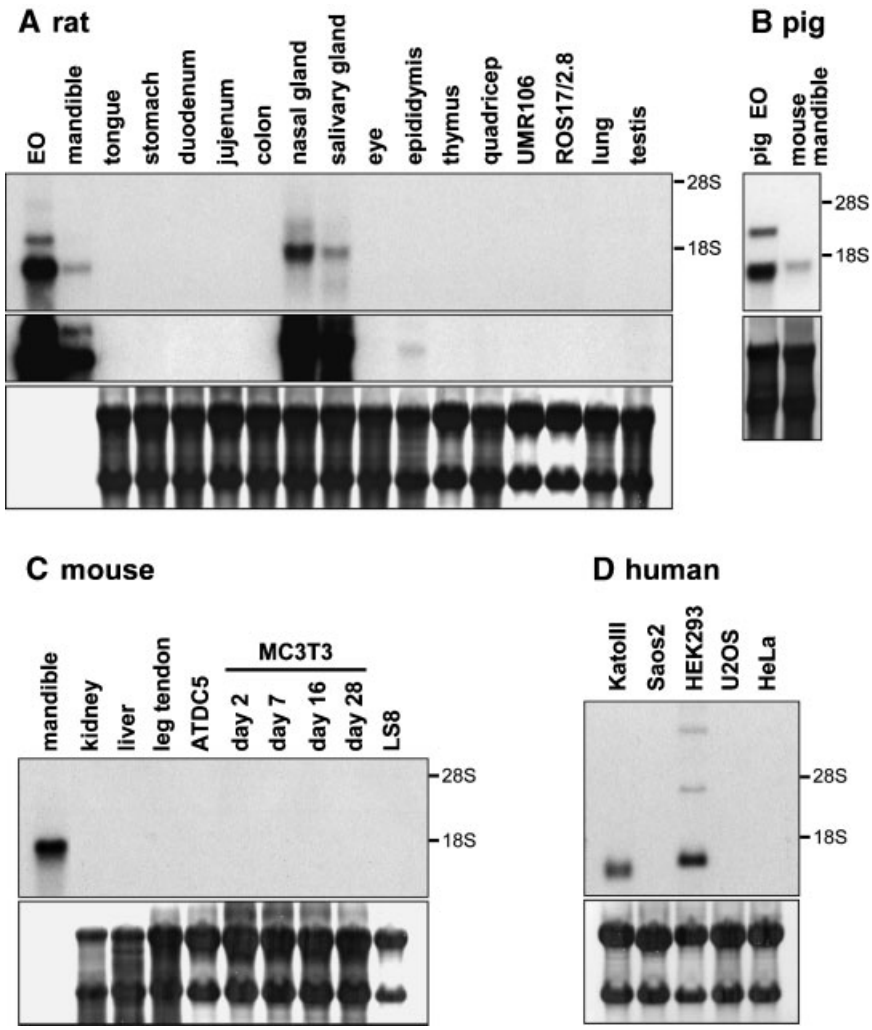

Fig. 1. Northern blot analyses of the expression of Apin in tissues and cells. Total RNA was extracted from adult tissues and/or cell lines of rat (**A**), pig (**B**), mice (**C**), and human (**D**) origin. Loads applied were 15 μg (A) or 10 μg (B–D) of RNA per lane and 0.3 μg per lane in the case of rat EO and mandible (A). RNA was also isolated from EOs at the maturation stage of development from mandibular incisors (A) and 3rd molars (B). In (A), the **middle panel** is a longer exposure of the same blot shown in the **top panel** and illustrates weak expression in epididymis. Integrity of RNA was monitored after staining the blots with methylene blue (**bottom panels**). Hybridization was carried out with species-specific Apin cDNA probes labeled with α^{32}P-dCTP. The positions of 28S and 18S ribosomal RNA are indicated.

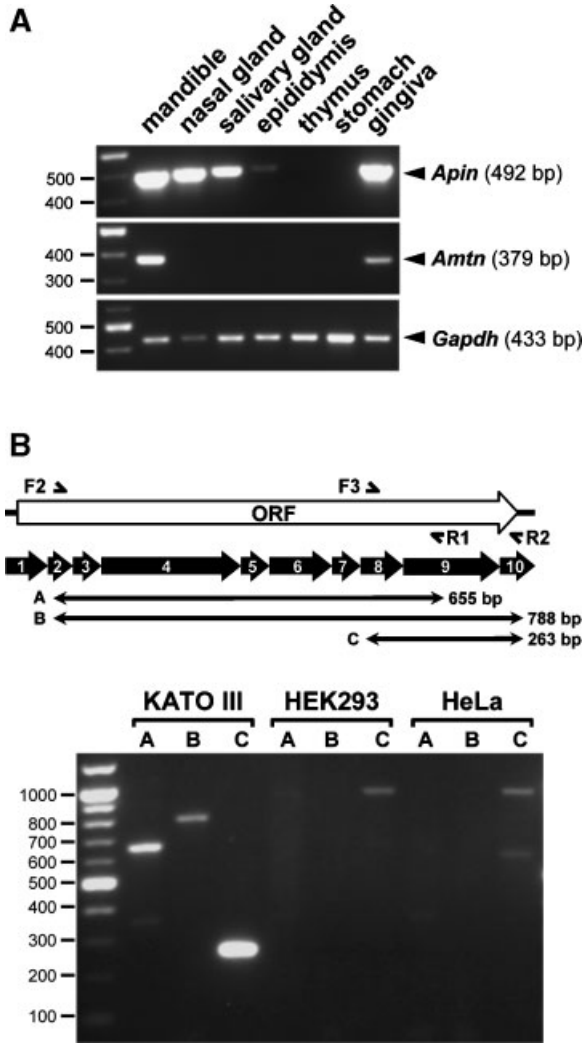

Fig. 2. RT-PCR analyses of Apin gene expression in rat and human. Total RNA was extracted from adult rat tissues (**A**) and human cell lines (**B**) and 250 ng used in one step RT-PCR. A: The rat Apin, Amtn, and Gapdh primers were used in parallel reactions and product sizes are indicated. PCR reactions were stopped after 26, 35, and 24 cycles for Apin, Amtn, and Gapdh, respectively. B: Three different human primer pairs were used each on the three cell lines. Only the KATOIII yielded the expected products as schematized. The PCR products were resolved on 1.5% agarose gels and stained with ethidium bromide. A 100 bp DNA ladder was used as markers.

gene structure with coding exons being phase 0 (Fig. 3). The Apin gene was not found in other species like fish, chicken, and frog, but it was present in several other mammals (elephant, hedgehog, armadillo) based on their preliminary genomic sequencing released at Ensembl. The overall identity between eight mammalian species was 43%, but reached 61% when only the N-terminal portions (residues 1–70) of the protein were considered. A signal sequence is present in all cases with the cleavage point by signal peptidase occurring after Ser[15] (Fig. 3). Except for several putative Ser/Thr/Tyr phosphorylation and O-linked glycosylation sites, most of which are conserved, no other obvious potential post-translational modifications could be predicted. At least in humans, two single nucleotide polymorphisms within the coding region were genotyped (Fig. 3, circled), one conserved for Leu[23] and another leading to an amino acid change Ile->Thr at position 222. Noticeable features of Apin common to all species is the absence of cysteine and the abundance of glutamine (17%), proline (11.8%), and leucine (9.4%) residues, expressed as frequency by weight.

Production of Bacterial 6His-Tagged Apin and Generation of a Polyclonal Antibody

In order to carry out immunolocalization experiments, a polyclonal antibody was generated against a bacterially produced rat Apin tagged at its N-terminus with six histidines (Fig. 4A). The protein was purified by Ni-affinity chromatography from the soluble extract after ultrasound disruption (Fig. 4B). The yield of the final preparation was roughly 35 mg for 2.5 L of starting bacterial culture. As judged by Coomassie blue staining after SDS–PAGE (Fig. 4B), a preponderant band migrating close to 30 kDa was attributed to the full length intact r6His-rApin for which the expected Mr was 29,332 kDa. LC-MS analyses confirmed the latter with an observed molecular mass of 29,335 kDa (Fig. 4C). Several smaller species visible on SDS–PAGE were also identified by LC-MS and corresponded to partial degradation products of the full length protein (Fig. 4C). The purity of r6His-rApin was estimated to be ~95%. Less abundant higher molecular weight bands (Fig. 3B, bracket) were immunoreactive with an anti-6His antibody (data not shown) suggesting partial aggregation of the r6His-rApin. In fact, upon longer storage at 22°C or 4°C, the recombinant Apin solutions tended to form white precipitates. Purified soluble protein was used for injections into rabbits according to standard immunization procedures (Affinity BioReagents) and the whole serum was collected.

Detection of Apin Produced by Transfected Cells

To test the rabbit antiserum, immunofluorescence detection was performed after

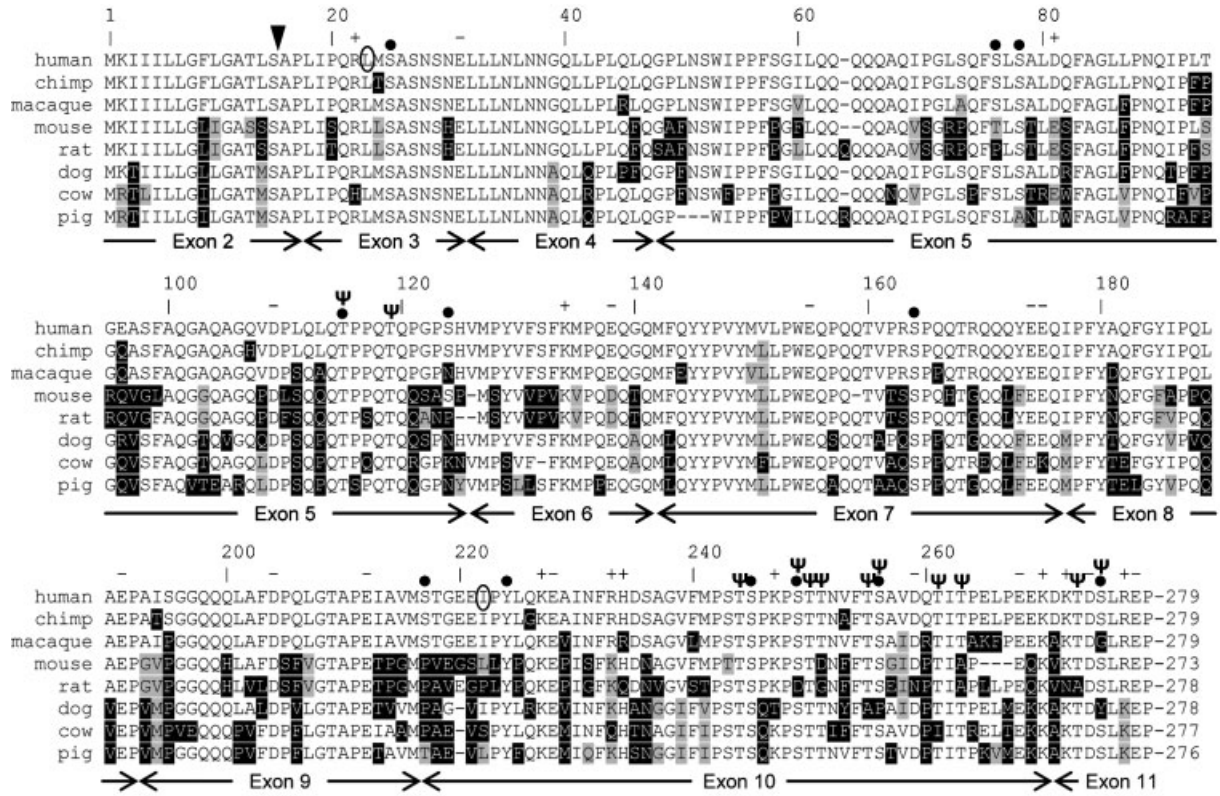

Fig. 3. Alignment of Apin sequences from various mammals. Numbering at top refers to the human sequence while those at the end indicate the total number of residues in each protein. Non-identical residues are highlighted in black, and similar ones in gray. The arrowhead indicates the point of cleavage of the signal peptide. Residues predicted to be phosphorylated (●) and/or O-glycosylated (Ψ) within the human protein are indicated. The coding exons numbered according to the rat gene, are illustrated at bottom. Two SNPs genotyped for the human are circled and conserved positively and negatively charged residues are indicated at the top. Sequences were obtained from GenBank entries EF113908 (human), DQ980195 (pig), EF121760 (cow), EF113909 (mouse), EF121758 (dog), (opossum), EF121761 (chimp), and EF121759 (macaque).

expression of rat Apin-FLAG by transient transfection in HEK293 and HeLa cells. When used at a 1:5,000 dilution, rat Apin was easily detected in the Golgi region of permeabilized cells (Fig. 5D,H, arrows), thus attesting of its presence in the secretory pathway. Labeling on intact HEK293 cells (Fig. 5C) produced a punctate signal (arrowheads) with occasional fibril-like pattern (arrows). Apin staining on intact HeLa cells was also punctate in appearance but more localized to what looked like peripherial cell membranes and intercellular junctions (Fig. 5G). Mock- or GFP-transfected cells showed no specific labeling irrespective of whether they were permeabilized or not (Fig. 5 A,B,E,F). Since the antibody was raised against rat Apin, we next verified its specificity against other species by Western blotting (Fig. 6A). Rat, pig, human, and mouse Apin were expressed in HEK293 after transfection and NP-40 detergent soluble cell extracts were prepared and separated by SDS–PAGE. Blotting with the antibody revealed specific bands at roughly the expected molecular weight for Apin precursor only for rat (Fig. 6A, white dot) and mouse (Fig. 6A, closed dot). Their migration pattern was much like that of the intact r6His-rApin (Fig. 6A, asterisk). The exsanguination antiserum used in Figure 6A also reacted non-specifically with several HEK293 cell extract proteins (bracket), but much less intense cross-reactions were noted with the first bleed antiserum used for subsequent Westerns (Fig. 6B–D). Immunofluorescence labeling performed on parallel samples showed only weak Golgi-like staining for the human Apin but not for the pig (data not shown). In another set of transfection experiments with HEK293 cells (Fig. 6B), FLAG-tagged rat Apin (rApin-FLAG) was readily detected by immunoblotting in the conditioned media collected from serum-free cultures (closed arrowhead). The apparent Mr of this secreted form of rApin-FLAG, however, was ~50 kDa which was considerably greater

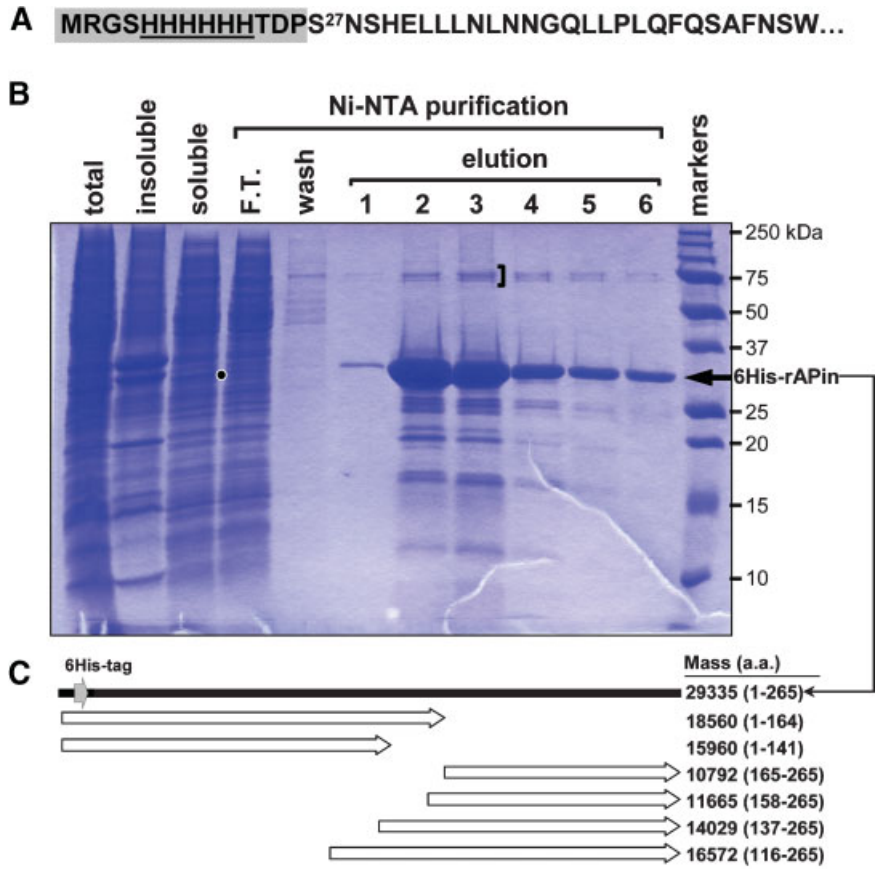

Fig. 4. Expression of rat Apin in bacteria and purification by nickel affinity chromatography. A cDNA fragment encoding rat Apin devoid of its native signal peptide (27–273) was subcloned in fusion with the 6-histidine tag of the pQE30 bacterial expression plasmid. The N-terminal portion of the expected recombinant protein is depicted (**A**). The M15 strain was used for production after induction with IPTG for 5 h. The soluble r6His-rApin protein was purified through Ni-NTA-agarose column and eluted with imidazole. Presence of r6His-rApin was monitored at each step on 8–16% SDS–PAGE gels and Coomassie blue staining (**B**). The final preparation contained the predominant full length r6His-rApin (Mr 29333) along with minor degradation products of which some could be assigned by mass spectrometry (**C**). [Color figure can be viewed in the online issue, which is available at www.interscience.wiley.com.]

than the theoretical mass of ~30 kDa expected on the basis of its amino acid sequence minus a signal peptide (Fig. 6B, open arrowhead). Cell extracts showed an immunoreactive band at the theoretical Mr expected for rApin-FLAG (Fig. 6B, open arrowhead), but this Mr was also almost identical to the 35 kDa non-specific band also present in the cells (Fig. 6A, base of bracket; Fig. 6B, mock, open arrowhead) thereby making conclusive identifications of the protein in cell extracts uncertain. Protein extracts prepared from rat and mouse tissues were also probed for Apin by Western blotting (Fig. 6C,D). Under the conditions used, only maturation stage EO segments from rat (Fig. 6C) and mouse (Fig. 6D) displayed a robust signal for Apin. In the rat, a diffuse band migrated between 40 and 47 kDa in the apical part of the maturation stage, which became more homogenous in size towards 47 kDa in the incisal segment (Fig. 6C, arrowheads). In the mouse, a similar pattern was observed with two species detected at 40 and 47 kDa but with increasing intensity from an apical to incisal direction (Fig. 6D, arrowheads). The results suggest that secreted Apin is post-translationally modified. In both maturation stage segments of rat, a band of weaker intensity co-migrating with r6His-rApin was also visible and could represent the unmodified Apin precursor (Fig. 6C, arrow). Immunoblotting for amelogenin revealed a unique band migrating at roughly 25 kDa mostly in secretory stage, which is the expected size and site for secretion of this protein.

Immunolocalization of Apin in Tissue Sections

The antibody was applied to immunolocalize the endogenous Apin protein on rat tissue sections

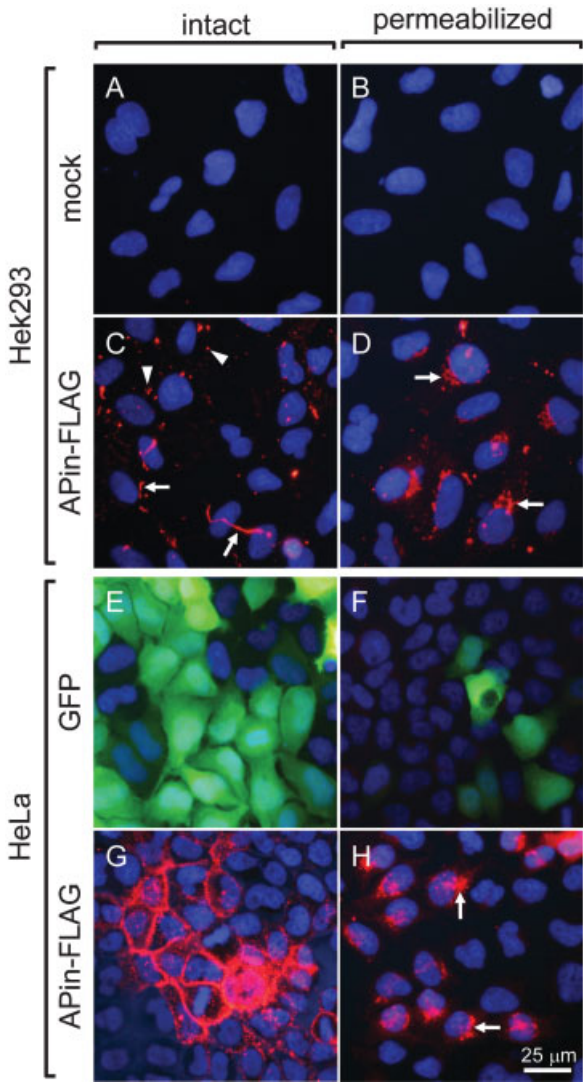

Fig. 5. Immunolocalization of rat Apin in transfected cells. HEK293 and HeLa cells were transfected with CMV-based expression plasmids encoding either rat Apin-FLAG, GFP, or the empty plasmid (mock). After 40 h, cells were processed for immunofluorescence visualization of Apin without (intact) or following permeabilization with Triton X-100. All cells were immunostained with the rabbit-anti-r6His-rApin antiserum followed by goat-anti-rabbit-Alexa594. GFP was monitored by its intense green autofluorescence. Nuclei were counterstained with Hoechst (blue). Notice the punctate and filamentous labeling in intact HEK293 cell cultures (**C**, arrows), and the pericellular labeling in HeLa cell cultures (**G**). Staining in the Golgi region was apparent in all permeabilized cells (**D**, **H**, arrows). Control incubations were devoid of signal (A, B, E, F). [Color figure can be viewed in the online issue, which is available at www.interscience.wiley.com.]

from incisors (Fig. 7) and molars (Fig. 8). Immunofluorescence pictures presented in Figure 7A illustrate localization of Apin in the rat lower incisor. In the EO, no specific signal was apparent from the apical portion of the incisor (data not shown) through to and including the entire secretory stage (Fig. 7B). Specific immunofluorescence signals only became visible starting in ameloblasts undergoing post-secretory transition (Fig. 7C). In the later region, a Golgi-like labeling pattern was observed in ameloblasts (Fig. 7C, open arrow), but a transient expression in the underlying papillary layer cells was also seen (Fig. 7C, closed arrow) which tapered off rapidly. At about the same time, Apin signals appeared in a punctate and broad line located at the interface between the ameloblasts and the enamel layer (Fig. 7C, arrowheads). The intensity of the signal at the apex of ameloblasts increased and persisted throughout the maturation stage (Fig. 7D) up to the gingival margin with a still prominent Golgi-like staining and with ruffle-ended cells generally showing a more intense apical reaction. For comparative purposes, the staining pattern for Amtn is shown (Fig. 7E); it appears as a characteristic thin and well-defined linear reaction associated with the basal lamina of ameloblasts and on the surface of the enamel layer where it artifactually detaches from the ameloblasts (EDTA-soluble region, Fig. 7A). Serial sections of maturation stage EO incubated with the pre-immune antiserum were devoid of specific signals (Fig. 7F). Noteworthy was the complete absence of staining within the enamel layer and connective tissue cells (Fig. 7A–D), as well as bone cells and matrix (not shown). A similar labeling pattern for Apin was observed on rat maxillary incisors and mouse mandibular incisors (not shown).

EOs from unerupted 3rd molars in development also showed strong labeling along the apices of maturation stage ameloblasts (Fig. 8A,B). Labeling was also detected on the JE at the level of both the interdental papilla and buccal and lingual sides of erupted molars in rats (Fig. 8C–F) and mice (not shown). Like the signal observed in the EO, the JE labeling appeared as a thin line at the interface between the cells and the enamel space (Fig. 8C–F, arrowheads) which extended from the cemento-enamel junction along the entire length of the JE. The reactivity however extended across the thickness of the JE and pericellular labeling was also evident (Fig. 8D,F, arrows). No specific signals were detected on the oral epithelium, connective tissues, and enamel layer (Fig. 8D). Among the thirteen other tissues tested, only duct cells in salivary and nasal glands, and

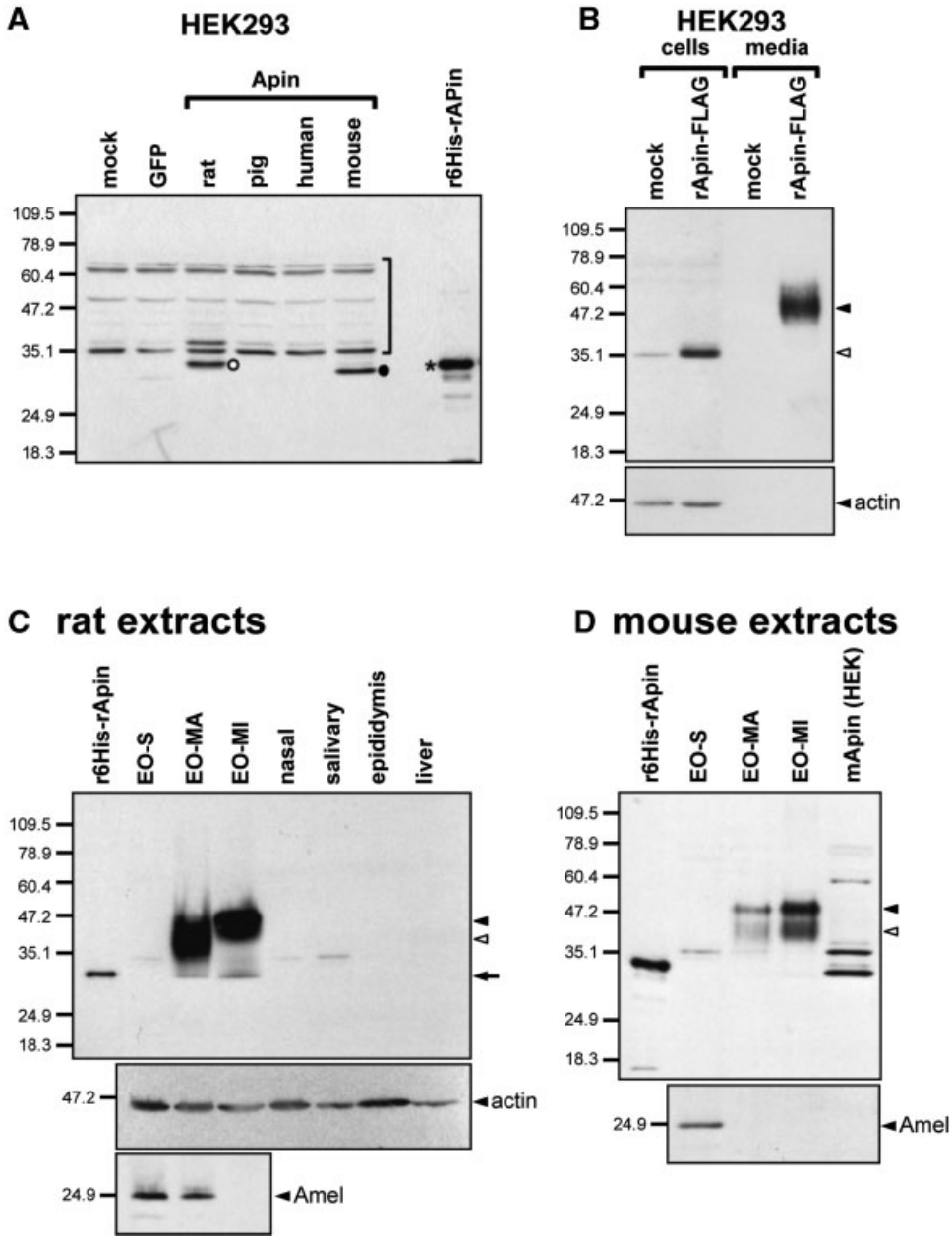

Fig. 6. Western blot detection of Apin in cells and tissues. **A**: This panel illustrates reactivity of anti-Apin antibody towards protein sequences derived from rat, pig, human, and mouse. Only Apin from rodents are detected in cell extracts after transient transfection of appropriate vectors in HEK293. Cells transfected with the empty vector (mock) or with a GFP vector served as controls. These revealed several proteins produced in HEK293 cross-react non-specifically (bracketed) with the antibody (see also last lane to right in **panel D**). Immunoblotting was performed with the rabbit antiserum raised against r6His-rApin that was loaded (0.5 ng) as a positive control. The computed molecular mass (in Da) of the detected proteins are 30,666 (rat, ○), 29,817 (mouse ●), 29,332 (r6His-rApin, *). **B**: This panel demonstrates that Apin is a secreted protein. In contrast to panel A, HEK293 cells in this case were transfected with a vector coding for a FLAG-tagged version of rat Apin (rApin-FLAG) which has a slightly higher base molecular weight (31,789 Da) than rat r6His-rApin (A). Transfected cells show an immunoreactive band near 35 kDa that is more intensely stained than the non-specific band also detected in mock cells (empty vector) at 35 kDa (open arrowhead). The secreted form of rApin-FLAG extracted from the media (closed arrowhead) has a molecular weight that is considerably greater than expected based on its theoretical mass (~30 kDa). The amount of protein loaded per lane represented 1/10th of a culture well. Immunoblotting for Apin in extracts from rat (**C**) and mouse (D) enamel organs (EO) and tissues. At least two forms (arrowheads) are detected in the apical (MA) and incisal (MI) segments of the maturation stage EO. In the rat (C), the Apin precursor is also weakly detected (arrow). As control, anti-amelogenin (Amel) reactivity was present mostly in the secretory stage (EO-S). Markers are indicated on the left.

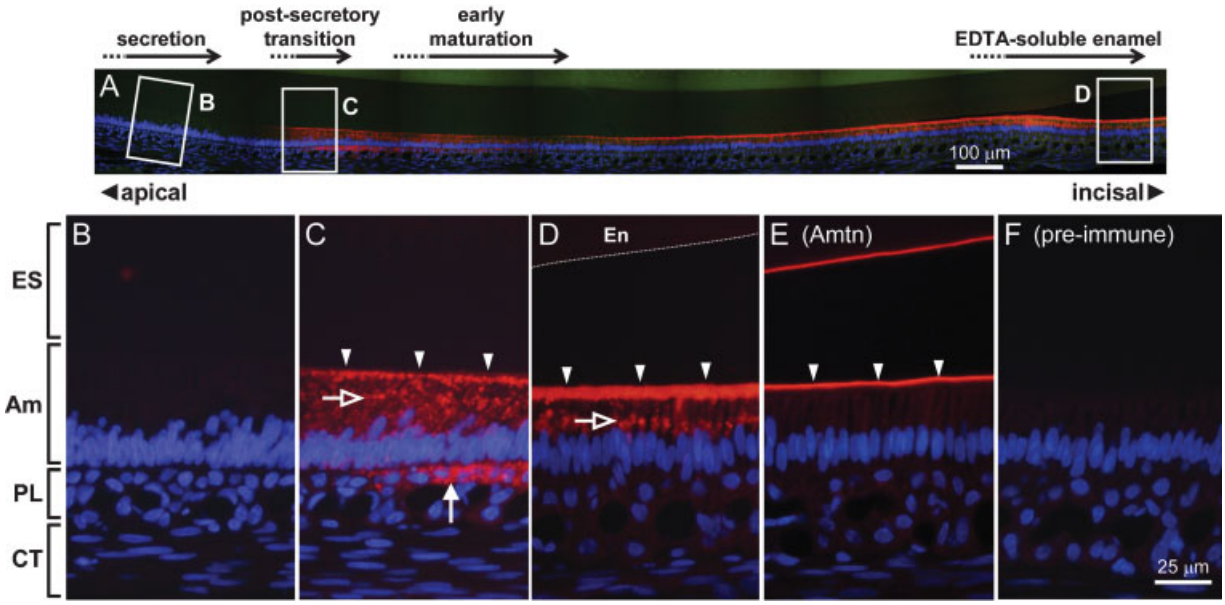

Fig. 7. Immunolocalization of Apin in the rat mandibular incisor. Composite image showing Apin localization (red staining) across a 2.2 mm long segment of a rat lower incisor enamel organ (EO) (**A**). Pictures in (**B**–**D**) are magnified regions boxed in (A). No specific signal is visible in secretory stage ameloblasts (Am) (B). Staining over the Golgi region of ameloblasts is apparent (arrow) in post-secretory transition (C) and throughout the maturation stage (D). Papillary layer cells (PL) display a transient expression of Apin only during post-secretory transition (C, upward arrow). Across the maturation stage, prominent and broad labeling is observed over ruffle-ended apical cell membranes of ameloblasts abutting a thin basal lamina at their surfaces (D, arrowheads). At this level of section (D), an artifactual EDTA-soluble space is present between the cells and the maturing enamel layer (En) (surface indicated by thin white dotted line). Anti-Amtn immunolabeling (**E**) on a serial section from the same area as panel D reveals the enamel basal lamina in two parts, as a thin red line along the surfaces of maturation ameloblasts and at the enamel surface which appears pulled away from the cells (E). Control incubations performed with pre-immune antisera were consistently unreactive (**F**). Sections were counterstained with Hoechst (blue); green coloration is tissue autofluorescence. ES, enamel space; CT, connective tissues; En, enamel.

principal and clear cells of epididymal ducts were immunoreactive (not shown).

DISCUSSION

We previously reported cloning of rat Apin and preliminary data concerning its gene structure and expression [Moffatt et al., 2006a]. Initial expression profiling in that study suggested that Apin might be restricted to maturation stage EOs. In the present study, mouse, human, and pig cDNAs have been cloned and used for expression analyses by Northern blotting, and these findings were confirmed by follow up RT-PCR characterizations. As documented herein, Apin is expressed at high levels in the teeth not only of rats, but also of mice and pigs. In rat, Apin mRNA signals are also detected at comparable levels in gingiva, and at moderate to low levels in nasal and salivary glands, and epididymis. The human gastric carcinoma KATOIII cell line expresses significant levels of Apin, which was confirmed by cloning of the full length cDNA comprising the entire open reading frame. In contrast, the positive signals detected in HEK293 cells by Northern blotting probably arise through aberrant transcripts as RT-PCR performed with three different primer pairs failed to detect expected specific products, all of which were present in KATOIII cells. Overall our data indicate that Apin has a broader expression spectrum than originally envisaged, which is consistent with experimental [Dey et al., 2001; Ozyildirim et al., 2005] and in silico data collected at Unigene (Hs.143811, Mm.389652). The expression data obtained here also agrees with previous reports of Apin expression in neoplasms of odontogenic [Solomon et al., 2003] and gastric [Aung et al., 2006] origins. It is intriguing that under certain pathological conditions Apin expression is upregulated. The possibility that Apin could represent a novel marker of certain cancers and the question of whether it has a causative role in the development or progression of the malignancy warrants further exploration. Certainly, these could represent suitable models to study

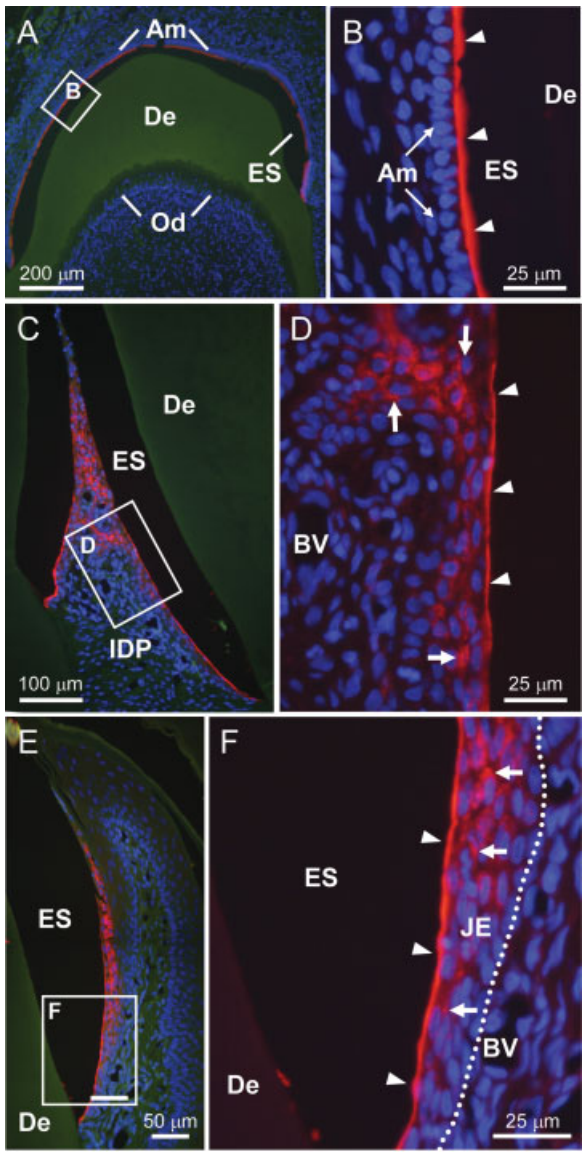

Fig. 8. Immunolocalization of Apin in rat mandibular molars. Immunofluorescence (red staining) detection of Apin in rat 3rd molar (**A**, **B**) and JE associated with erupted 1st and 2nd molars (**C**, **F**). Magnified views (**D**, F) of areas boxed in (C and **E**), respectively. Apin immunolabeling is present along the interface between the enamel organ and developing enamel in unerupted 3rd molar (B) and between junctional epithelium (JE) and mature enamel (D, F, arrowheads) around the cervical regions of 1st and 2nd molars. Expression is also detected (arrows) within deeper cell layers of the epithelium in areas of the interdental papilla (IDP) (C, D) and buccal and lingual sides of 2nd molars (E, F). Sections were counterstained with Hoechst (blue). Green coloration is tissue autofluorescence. ES, enamel space; Am, ameloblasts; De, dentin; BV, blood vessels.

signal transduction pathways mechanisms that lead to deregulated and unrestrained gene activation.

The antibody made to recombinant rat Apin was found to be very effective at detecting native rat and mouse proteins both by Western blotting and immunohistochemistry. Its poor reactivity against human and pig proteins, however, is accounted for by the overall lower homology to the rat sequence (66% and 62%, respectively). Nevertheless, positive immunoreactivity of human Apin in the Golgi of transfected cells (data not shown) indicates that the antibody can recognize the human protein if expression levels are high and/or the protein is concentrated at specific sites. This is likely the case in CEOT where positive immunohistochemical labelings with the antibody to the rat protein reveal the presence of Apin in the amorphous amyloid deposits (data not shown), as previously reported by Solomon et al. [2003].

Both bacterial recombinant Apin and the intracellular form of Apin extracted directly from cells migrate on SDS–PAGE gels very near the theoretical molecular mass expected for the protein lacking a signal peptide. Secreted Apin isolated from conditioned media of cell cultures or from mouse and rat EOs, however, had an apparent molecular weight that was roughly +20 kDa higher. This increase in molecular weight is most likely due to post-translational modifications occurring on the many predicted sites for phosphorylation and O-glycosylation. Another possibility, although less likely, is that Apin could be crosslinked to a small (+20 kDa) partner protein, perhaps through the action of tissue transglutaminase [Nurminskaya and Kaartinen, 2006]. Indeed, such enzymes are known to be expressed in oral mucosa and believed to participate in maintaining epithelial tissue and cell integrity [Presland and Dale, 2000]. Self aggregation may also contribute to increasing the apparent molecular weight of a protein, but this is deemed unlikely in this case since the electrophoretic profile of native secreted Apin does not show the multiband laddering pattern typical of proteins prone to extensive oligomerization [Podlisny et al., 1995], and aggregates would have shown increases equivalent to +29 kDa as opposed to the +20 kDa actually observed. Analysis of the amino acid sequence of Apin by algorithms that estimates the propensity for cross β-aggregation [Fernandez-Escamilla et al., 2004; Conchillo-Sole et al., 2007] indicated weak tendencies relative to residues 126–130 (MSYVV) and 147–151 (VYMLL) in the secreted protein. Preliminary evidence suggests that the amyloidogenic potential of Apin in CEOT corresponds

to a region of the protein encompassing these two domains [Foster et al., 2006].

Immunolocalizations on sections from rat and mouse teeth confirmed expression data that Apin signals are restricted to the maturation stage of amelogenesis. They additionally revealed that the protein is manufactured by ameloblasts and, except for a brief moment in time, not by cells forming the papillary layer of the EO. The localization pattern observed for Apin was reminiscent of another protein, Amtn [Iwasaki et al., 2005; Moffatt et al., 2006b], that was also identified by screening the EO secretome [Moffatt et al., 2006a]. There are some notable differences however in the immunolabeling patterns for these two proteins. Like Amtn, Apin is first detected at the start of the maturation stage (postsecretory transition) where ameloblasts exhibit reactivity both in the Golgi region and at their apical surfaces. The Golgi-like staining for Apin persists throughout the maturation stage up to the gingival margin while that for Amtn becomes fainter soon after ameloblasts progress into maturation. Another difference is that staining for Apin along the apical surfaces of ameloblasts is more diffuse than Amtn which localizes precisely to the thin basal lamina mediating the attachment of the EO to the tooth surface [Moffatt et al., 2006b]. The other notable site of expression for both Apin and Amtn is the JE surrounding erupted teeth. Here again the localization of Amtn was well-defined and associated with the basal lamina present on the enamel surface [Moffatt et al., 2006b] while staining for Apin is present both at the outer surface of flattened superficial squamous cells as well as throughout all of the cell layers forming the stratified JE. The colocalization of Apin and Amtn suggests that both have a role in mediating the adhesion of epithelia to the tooth surface and raises the possibility that they may interact with each other to achieve this function. Protein interaction studies with recombinant proteins or using the yeast two-hybrid system could provide some information on this possibility. However, the presence of Apin among cells of the JE in a manner reminiscent to surface staining on transfected HeLa cells, and its expression at non-dental sites such as excretory ducts of nasal and salivary glands, and epithelial cells lining the epidydimal ducts suggest that this unique protein may have multiple functions beyond mediating cell–matrix adhesion. One common feature of the maturation stage EO, JE and duct cells is that they are all involved in creating and maintaining differential microenvironments between apical and basal compartments including distinctive pH and ionic compositions. Substantial exchange of material occurs between these compartments and sustaining a cohesive cell layer is indispensable in this activity.

While this manuscript was in review, Park et al. [2007] published a paper reporting by in situ hybridization that Apin is highly expressed by maturation stage ameloblasts and weakly by secretory ameloblasts. Using an anti-peptide antibody, they detected intense Apin immunostaining in the Golgi and at the apex of ruffle-ended maturation stage ameloblast. They further reported strong Apin immunostaining in JE. Weak immunostaining was also described along the Tomes' processes of secretory ameloblasts [Park et al., 2007]. Our results are in good agreement with most of these observations except regarding secretory stage ameloblasts and Tomes' processes which never appeared immunoreactive using an antibody raised against recombinant rat Apin as antigen. While these differences in results clearly could relate to the different types of antibodies used (synthetic peptide versus whole recombinant protein), it is equally possible that the labeling of Apin we classified as localized to post-secretory transition (Fig. 7C) might correspond to the same region adjacent to the start of maturation proper that Park et al. [2007] classified as part of the secretory stage. Potential post-translational modifications of secreted Apin was noted by Park et al. [2007], but the large 20 kDa shift in molecular weight we observed for Apin in Western blots of proteins extracted from in vitro and in vivo sources (Fig. 6) was not found by Park et al. [2007] in their culture system. This could be related to differences in the cell types used for in vitro studies (C2C12 vs. HEK293), as was previously found with Amtn [Iwasaki et al., 2005; Moffatt et al., 2006b]. The observations made both in the present study and by Park et al. [2007] that Apin signals at the apex of ameloblasts change between ruffle and smooth-ended phases are definitely very pertinent to a potential role related to ameloblast modulation. Based on in vitro expression data with an immortalized ameloblast cell line, Park et al. [2007] concluded that Apin is involved in mineralization and maturation of enamel,

possibly in part by up regulating expression of MMP-20 and tuftelin. While these suggestions are interesting and definitely merit further consideration, their pertinence to events occurring in vivo is questionable since MMP-20 is produced by ameloblasts primarily during the secretory stage of amelogenesis [Fukae et al., 1998], when Apin expression is weak [Park et al., 2007] or nonexistent (this paper), and tuftelin lacks a signal peptide [MacDougall et al., 1998] and therefore is not a secretory product of ameloblasts with regulatory controls comparable to MMP20 and Apin.

In summary, we have determined that Apin, a secreted protein until now associated with neoplastic transformation, is highly expressed in maturation stage EO and JE cells, and at lower levels in the nasal and salivary glands, and epidydimis. In the tooth, the protein is conspicuous by its accumulation at the surface of the EO and JE cells where it may mediate their adhesion to the tooth surface. However, the presence of Apin among cells of the JE suggests that, unlike Amtn, its activity goes beyond interacting with mineralized surfaces. Its expression by epithelia tissues possessing distinctly different functions and its upregulation in certain neoplasms further indicate that Apin likely has more than one physiological role.

ACKNOWLEDGMENTS

This work was supported by the Canadian Institutes of Health Research. We are grateful to Micheline Fortin for her expert technical assistance with tissue processing, sectioning, and immunolabeling.

REFERENCES

Aung PP, Oue N, Mitani Y, Nakayama H, Yoshida K, Noguchi T, Bosserhoff AK, Yasui W. 2006. Systematic search for gastric cancer-specific genes based on SAGE data: Melanoma inhibitory activity and matrix metalloproteinase-10 are novel prognostic factors in patients with gastric cancer. Oncogene 25:2546–2557.

Bartlett JD, Ganss B, Goldberg M, Moradian-Oldak J, Paine ML, Snead ML, Wen X, White SN, Zhou YL. 2006. 3. Protein-protein interactions of the developing enamel matrix. Curr Top Dev Biol 74:57–115.

Bonass WA, Kirkham J, Shore RC, Brookes SJ, Godfrey CL, Robinson C. 1998. Identification of rat enamel organ RNA transcripts using differential-display. Connect Tissue Res 38:249–256.

Caterina JJ, Skobe Z, Shi J, Ding Y, Simmer JP, Birkedal-Hansen H, Bartlett JD. 2002. Enamelysin (matrix metalloproteinase 20)-deficient mice display an amelogenesis imperfecta phenotype. J Biol Chem 277:49598–49604.

Chen LS, Couwenhoven RI, Hsu D, Luo W, Snead ML. 1992. Maintenance of amelogenin gene expression by transformed epithelial cells of mouse enamel organ. Arch Oral Biol 37:771–778.

Church GM, Gilbert W. 1984. Genomic sequencing. Proc Natl Acad Sci USA 81:1991–1995.

Conchillo-Sole O, de Groot NS, Aviles FX, Vendrell J, Daura X, Ventura S. 2007. AGGRESCAN: A server for the prediction and evaluation of "hot spots" of aggregation in polypeptides. BMC Bioinformatics 8:65.

Dey R, Son HH, Cho MI. 2001. Isolation and partial sequencing of potentially odontoblast-specific/enriched rat cDNA clones obtained by suppression subtractive hybridization. Arch Oral Biol 46:249–260.

Fernandez-Escamilla AM, Rousseau F, Schymkowitz J, Serrano L. 2004. Prediction of sequence-dependent and mutational effects on the aggregation of peptides and proteins. Nat Biotechnol 22:1302–1306.

Flenniken AM, Osborne LR, Anderson N, Ciliberti N, Fleming C, Gittens JE, Gong XQ, Kelsey LB, Lounsbury C, Moreno L, Nieman BJ, Peterson K, Qu D, Roscoe W, Shao Q, Tong D, Veitch GI, Voronina I, Vukobradovic I, Wood GA, Zhu Y, Zirngibl RA, Aubin JE, Bai D, Bruneau BG, Grynpas M, Henderson JE, Henkelman RM, McKerlie C, Sled JG, Stanford WL, Laird DW, Kidder GM, Adamson SL, Rossant J. 2005. A Gja1 missense mutation in a mouse model of oculodentodigital dysplasia. Development 132:4375–4386.

Foster JS, Kestler DP, Murphy CL, Kennel SJ, Wall JS, Weiss DT, Solomon A. 2006. Amyloidogenic region of odontogenic ameloblast associated protein (ODAM). Amyloid 13(Suppl 1):28–29.

Fukae M, Tanabe T, Uchida T, Lee SK, Ryu OH, Murakami C, Wakida K, Simmer JP, Yamada Y, Bartlett JD. 1998. Enamelysin (matrix metalloproteinase-20): Localization in the developing tooth and effects of pH and calcium on amelogenin hydrolysis. J Dent Res 77:1580–1588.

Fukumoto S, Kiba T, Hall B, Iehara N, Nakamura T, Longenecker G, Krebsbach PH, Nanci A, Kulkarni AB, Yamada Y. 2004. Ameloblastin is a cell adhesion molecule required for maintaining the differentiation state of ameloblasts. J Cell Biol 167:973–983.

Gibson CW, Yuan ZA, Hall B, Longenecker G, Chen E, Thyagarajan T, Sreenath T, Wright JT, Decker S, Piddington R, Harrison G, Kulkarni AB. 2001. Amelogenin-deficient mice display an amelogenesis imperfecta phenotype. J Biol Chem 276:31871–31875.

Hart PS, Hart TC, Michalec MD, Ryu OH, Simmons D, Hong S, Wright JT. 2004. Mutation in kallikrein 4 causes autosomal recessive hypomaturation amelogenesis imperfecta. J Med Genet 41:545–549.

Huq NL, Cross KJ, Ung M, Reynolds EC. 2005. A review of protein structure and gene organisation for proteins associated with mineralised tissue and calcium phosphate stabilisation encoded on human chromosome 4. Arch Oral Biol 50:599–609.

Iwasaki K, Bajenova E, Somogyi-Ganss E, Miller M, Nguyen V, Nourkeyhani H, Gao Y, Wendel M, Ganss B. 2005. Amelotin—A novel secreted, ameloblast-specific protein. J Dent Res 84:1127–1132.

Kawasaki K, Weiss KM. 2003. Mineralized tissue and vertebrate evolution: The secretory calcium-binding

phosphoprotein gene cluster. Proc Natl Acad Sci USA 100:4060–4065.
Kawasaki K, Weiss KM. 2006. Evolutionary genetics of vertebrate tissue mineralization: The origin and evolution of the secretory calcium-binding phosphoprotein family. J Exp Zoolog B Mol Dev Evol 306:295–316.
Kinane DF, Shiba H, Hart TC. 2005. The genetic basis of periodontitis. Periodontol 2000 39:91–117.
Lal A, Lash AE, Altschul SF, Velculescu V, Zhang L, McLendon RE, Marra MA, Prange C, Morin PJ, Polyak K, Papadopoulos N, Vogelstein B, Kinzler KW, Strausberg RL, Riggins GJ. 1999. A public database for gene expression in human cancers. Cancer Res 59:5403–5407.
MacDougall M, Simmons D, Dodds A, Knight C, Luan X, Zeichner-David M, Zhang C, Ryu OH, Qian Q, Simmer JP, Hu CC. 1998. Cloning, characterization, and tissue expression pattern of mouse tuftelin cDNA. J Dent Res 77:1970–1978.
Masuya H, Shimizu K, Sezutsu H, Sakuraba Y, Nagano J, Shimizu A, Fujimoto N, Kawai A, Miura I, Kaneda H, Kobayashi K, Ishijima J, Maeda T, Gondo Y, Noda T, Wakana S, Shiroishi T. 2005. Enamelin (Enam) is essential for amelogenesis: ENU-induced mouse mutants as models for different clinical subtypes of human amelogenesis imperfecta (AI). Hum Mol Genet 14:575–583.
Miskin R, Masos T, Shoham Z, Williams-Simons L. 2006. Urokinase-type plasminogen activator mRNA is expressed in normal developing teeth and leads to abnormal incisor enamel in alphaMUPA transgenic mice. Transgenic Res 15:241–254.
Moffatt P, Salois P, St-Amant N, Gaumond MH, Lanctot C. 2004. Identification of a conserved cluster of skin-specific genes encoding secreted proteins. Gene 334:123–131.
Moffatt P, Smith CE, Sooknanan R, St-Arnaud R, Nanci A. 2006a. Identification of secreted and membrane proteins in the rat incisor enamel organ using a signal-trap screening approach. Eur J Oral Sci 114 (Suppl 1):139–146.
Moffatt P, Smith CE, St-Arnaud R, Simmons D, Wright JT, Nanci A. 2006b. Cloning of rat amelotin and localization of the protein to the basal lamina of maturation stage ameloblasts and junctional epithelium. Biochem J 399: 37–46.
Moradian-Oldak J, Paine ML, Lei YP, Fincham AG, Snead ML. 2000. Self-assembly properties of recombinant engineered amelogenin proteins analyzed by dynamic light scattering and atomic force microscopy. J Struct Biol 131:27–37.
Nurminskaya M, Kaartinen MT. 2006. Transglutaminases in mineralized tissues. Front Biosci 11:1591–1606.
Orsini G, Lavoie P, Smith C, Nanci A. 2001. Immunochemical characterization of a chicken egg yolk antibody to secretory forms of rat incisor amelogenin. J Histochem Cytochem 49:285–292.
Ozyildirim AM, Wistow GJ, Gao J, Wang J, Dickinson DP, Frierson HF Jr, Laurie GW. 2005. The lacrimal gland transcriptome is an unusually rich source of rare and poorly characterized gene transcripts. Invest Ophthalmol Vis Sci 46:1572–1580.
Park JC, Park JT, Son HH, Kim HJ, Jeong MJ, Lee CS, Dey R, Cho ML. 2007. The amyloid protein APin is highly expressed during enamel mineralization and maturation in rat incisors. Eur J Oral Sci 115:153–160.
Philipsen HP, Reichart PA. 2000. Calcifying epithelial odontogenic tumour: Biological profile based on 181 cases from the literature. Oral Oncol 36:17–26.
Podlisny MB, Ostaszewski BL, Squazzo SL, Koo EH, Rydell RE, Teplow DB, Selkoe DJ. 1995. Aggregation of secreted amyloid beta-protein into sodium dodecyl sulfate-stable oligomers in cell culture. J Biol Chem 270:9564–9570.
Presland RB, Dale BA. 2000. Epithelial structural proteins of the skin and oral cavity: Function in health and disease. Crit Rev Oral Biol Med 11:383–408.
Rios H, Koushik SV, Wang H, Wang J, Zhou HM, Lindsley A, Rogers R, Chen Z, Maeda M, Kruzynska-Frejtag A, Feng JQ, Conway SJ. 2005. Periostin null mice exhibit dwarfism, incisor enamel defects, and an early-onset periodontal disease-like phenotype. Mol Cell Biol 25: 11131–11144.
Rosty C, Aubriot MH, Cappellen D, Bourdin J, Cartier I, Thiery JP, Sastre-Garau X, Radvanyi F. 2005. Clinical and biological characteristics of cervical neoplasias with FGFR3 mutation. Mol Cancer 4:15.
Ryan MC, Lee K, Miyashita Y, Carter WG. 1999. Targeted disruption of the LAMA3 gene in mice reveals abnormalities in survival and late stage differentiation of epithelial cells. J Cell Biol 145:1309–1323.
Smith CE. 1998. Cellular and chemical events during enamel maturation. Crit Rev Oral Biol Med 9:128–161.
Smith CE, Nanci A, Moffatt P. 2006. Evidence by signal peptide trap technology for the expression of carbonic anhydrase 6 in rat incisor enamel organs. Eur J Oral Sci 114 (Suppl 1):147–153.
Solomon A, Murphy CL, Weaver K, Weiss DT, Hrncic R, Eulitz M, Donnell RL, Sletten K, Westermark G, Westermark P. 2003. Calcifying epithelial odontogenic (Pindborg) tumor-associated amyloid consists of a novel human protein. J Lab Clin Med 142:348–355.
Sui W, Boyd C, Wright JT. 2003. Altered pH regulation during enamel development in the cystic fibrosis mouse incisor. J Dent Res 82:388–392.
The FANTOM Consortium. 2005. The transcriptional landscape of the mammalian genome. Science 309: 1559–1563.
Thomas G, Moffatt P, Salois P, Gaumond MH, Gingras R, Godin E, Miao D, Goltzman D, Lanctot C. 2003. Osteocrin, a novel bone-specific secreted protein that modulates the osteoblast phenotype. J Biol Chem 278: 50563–50571.
Wilkinson M, Doskow J, Lindsey S. 1991. RNA blots: Staining procedures and optimization of conditions. Nucleic Acids Res 19:679.
Wright JT. 2006. The molecular etiologies and associated phenotypes of amelogenesis imperfecta. Am J Med Genet A 140A:2547–2555.